



# Fabrication of impressive electrically conductive Cu–Ti<sub>2</sub>SnC composite wires through the friction stir back extrusion process

Amirhossein Jahani<sup>1</sup> · Hamed Jamshidi Aval<sup>1</sup> · Mohammad Rajabi<sup>1</sup> · Roohollah Jamaati<sup>1</sup>

Received: 10 October 2022 / Accepted: 16 February 2023 / Published online: 4 April 2023  
© The Author(s), under exclusive licence to The Brazilian Society of Mechanical Sciences and Engineering 2023

## Abstract

This paper investigates the effect of extrusion speed on the microstructure, mechanical, electrical, and wear properties of Cu–8 wt%Ti<sub>2</sub>SnC composite wires fabricated through friction stir back extrusion. The results showed that a layered structure was formed in the surface areas of the composite wire as the extrusion speed decreased from 85 to 25 mm/min. The friction stir back extrusion on primary composite results in grain size reduction from  $8.34 \pm 0.89$  to  $4.23 \pm 0.95$   $\mu\text{m}$ . Also, increasing the extrusion speed from 25 to 85 mm/min decreased the decomposition of Ti<sub>2</sub>SnC and the formation of the Cu<sub>81</sub>Sn<sub>22</sub> phase. The smaller grain size and higher concentration of Ti<sub>2</sub>SnC reinforcement surrounding the composite wire resulted in higher hardness at this zone than in the central areas of wires. In addition, the addition of 8 wt% Ti<sub>2</sub>SnC reinforcement and performing FSBE at a rotational speed of 1000 rpm and a traverse speed of 85 mm/min increased the yield strength and UTS by 161 and 33%, respectively, compared to the un-reinforced copper matrix. It was observed that increasing the extrusion speed from 25 to 85 mm/min improved the MAX phase/Cu matrix interface quality and the distribution of MAX phases, thus causing the wear rate to decrease from 0.0067 to 0.0048 mg/m and electrical conductivity to increase from 64.32 to 76.89%IACS.

**Keywords** Cu–Ti<sub>2</sub>SnC composite · Friction stir back extrusion · Microstructure · Electrical conductivity · Wear resistance

## 1 Introduction

Copper has good ductility, excellent thermal-electrical conductivity, relatively low price, and attractive corrosion properties, as well as good weldability, and castability [1]. However, its weak mechanical properties limit its applications [2, 3]. Similar to what has been reported about metal matrix composites [4, 5], one of the ways to improve the mechanical properties and wear resistance of copper is to reinforce it with dispersed particles to produce copper matrix composites (CMCs) [6]. These reinforcements can result in thermodynamic and chemical stability, low diffusion and solubility in the copper matrix, and high interface energy between the particle and matrix [7]. Different ceramic particles, such as

TiB<sub>2</sub>, SiC, and Al<sub>2</sub>O<sub>3</sub>, and intermetallic compounds, such as Al<sub>3</sub>Ti and Ni<sub>3</sub>Al, have been used as copper reinforcements.

The use of these materials weakens the electrical conductivity and toughness due to poor interfacial bonding [8]. Some reinforcements do not provide the required wear properties. Another group of materials that are used as reinforcing particles in metal matrix composites is MAX phases or ternary carbides. Ternary carbides or MAX phases with extraordinary physical and mechanical properties combine the advantages of metals and ceramics. These materials are hexagonal structures with the general formula M<sub>n+1</sub>AX<sub>n</sub>, where n is from 1 to 3, M is a transition metal, A is an element from groups 13 to 16 of the periodic table, and X is carbon or nitrogen. Unlike binary carbides, which are very hard and brittle, MAX phases are semi-plastic materials with high strength. They are also resistant to creep, fatigue, and corrosion and have an extremely low coefficient of friction. The mechanical properties of MAX phases include a bending strength of 300–500 MPa and a fracture toughness of 5–7 MPa.m<sup>1/2</sup>. These good properties have extended their application [9]. The mentioned characteristics make MAX phase particles suitable reinforcing agents in the construction of CMCs.

Technical Editor: Lincoln Cardoso Brandao.

✉ Hamed Jamshidi Aval  
h.jamshidi@nit.ac.ir

<sup>1</sup> Department of Materials Engineering, Babol Noshirvani University of Technology, Shariati Avenue, Babol 47148-71167, Iran

The unique characteristics of MAX phases give CMCs high electrical and mechanical properties, turning them into promising candidates for advanced electrical applications, such as spot-welding electrodes, high-performance electrical switches, neutron rotating target supports, brushes, design of radiators and cylinder heads, electric discharge machining electrodes, liners and disk brakes, dry sliding materials, anticorrosive coatings, and heat sinks and spreaders.

Ti<sub>3</sub>SiC<sub>2</sub>, Ti<sub>3</sub>AlC<sub>2</sub>, and Ti<sub>2</sub>SnC particles have been used in the fabrication of CMCs [10]. Ti<sub>2</sub>SnC has the highest electrical conductivity among MAX phases ( $14 \times 10^6 \Omega^{-1} \text{ m}^{-1}$ ) [11]. It has been demonstrated that adding one volume percent of Ti<sub>2</sub>SnC as reinforcement to Cu–Ti<sub>2</sub>SnC composites fabricated by the powder metallurgy method gives them an electrical conductivity of about 85.6% of pure copper [10]. The fabrication of Cu–Ti<sub>2</sub>SnC composite has been reported in a limited number of studies. Wu et al. [10, 12–14] studied the microstructure and mechanical properties of a hot-pressed Cu–Ti<sub>2</sub>SnC composite. The results showed that the addition of the MAX phase significantly reduced the grain size and wear rate compared to the sample without reinforcement, and the addition of 5 vol% of the MAX phase increased the yield strength to 188 MPa. Zhang et al. [15] reported that by increasing the amount of Ti<sub>2</sub>SnC reinforcement, especially up to 5 wt%, the hardness of the composite increased considerably. This is while they also reported that by adding more reinforcement, not only the strength and hardness but also the wear rate did not show a significant increase. The hot-pressing method has been used in all studies on Ti<sub>2</sub>SnC-reinforced CMC production. In this method, due to the decomposition of the Ti<sub>2</sub>SnC phase at high temperatures and times, the entire porosity cannot be eliminated to achieve high density. However, porosity causes the formation of stress concentration positions and weakens the mechanical and physical properties of the CMC.

In this research, the aim was to achieve a composite with high density and uniform structure with minimal possibility of decomposition of the reinforcing phase during processing by friction stir back extrusion (FSBE) and applying severe plastic deformation (SPD) during the process. Although the production of metallic or metal matrix composite wire using the FSBE method has been studied previously [16, 17], the effect of the extrusion speed of the FSBE process on the properties of CMC wire has not been investigated. Accordingly, here, the effects of the extrusion speed of the FSBE process on the microstructure, mechanical properties, electrical conductivity, and wear resistance of CMC wires reinforced with 8 wt% of Ti<sub>2</sub>SnC were studied.

## 2 Experimental procedures

Figure 1 demonstrates the steps for the fabrication of the Cu–Ti<sub>2</sub>SnC composite using the FSBE method. At first, copper powder with a purity of 99.9% and an average particle size of 5 μm and Ti<sub>2</sub>SnC powder with a purity of 99.9% and an average particle size of 15 μm were mixed to make CMC with 8 wt% of the MAX phase. In order to homogenize this mixture, a mechanical stirrer with steel balls was used at a ball-to-material ratio of 5:1. The powder mixture was pressed into a cylindrical mold with a diameter and height of 20 and 40 mm under a pressure of 150 bar. As shown in Fig. 1, before the extrusion process, the preformed composite samples were sintered at 850 °C for 30 min under argon gas atmosphere protection. The extrusion parameters were selected based on preliminary investigations on rotational speed in the range of 400–1200 rpm and the extrusion speed of 45 mm/min. Since the best mechanical properties, electrical conductivity, and wear resistance were obtained at the rotational speed of 1000 rpm, this rotational speed was used to continue the research. In this research, the effect of traverse speed in the range of 25–85 mm/min at a constant rotational speed of 1000 rpm was studied. Table 1 specifies the different labels used for the samples.

After extrusion, different samples were prepared to check the microstructure, mechanical properties, wear resistance, and electrical conductivity. Figure 2 displays the prepared samples along with the dimensions to check the various properties. In order to investigate the microstructure of the composite wire cross section, it was prepared using SiC sandpaper and alumina suspension. Then, using a reagent composed of 85 ml distilled water, 15 ml HCl, and 5 g FeCl<sub>3</sub> the cross section of the samples was etched to reveal the microstructure. The microstructure was examined using the NGF–120A optical microscope and a Philips-XL30FSEM scanning electron microscope (SEM) equipped with an EDS detector. In addition, a Rigaku Ultima IV X-ray diffraction machine was used for phase analysis. The hardness of the samples was measured using a KOOPA Universal (UV1) microhardness tester with a force of 100 gr and a duration time of 15 s. The tensile test was performed according to the ASTM E8 standard using a crosshead speed of 1 mm/min. The electrical conductivity test was performed on different samples according to the ASTM F1711 standard. The wear test was performed according to the ASTM G99 standard using pin on disk method. The counterface was made of steel with a hardness of 60 HRC. The wear test was carried out under a load of 20 N at a distance of 2000 m. After the tensile and wear test, the fracture and wear surfaces of the samples were examined by SEM.

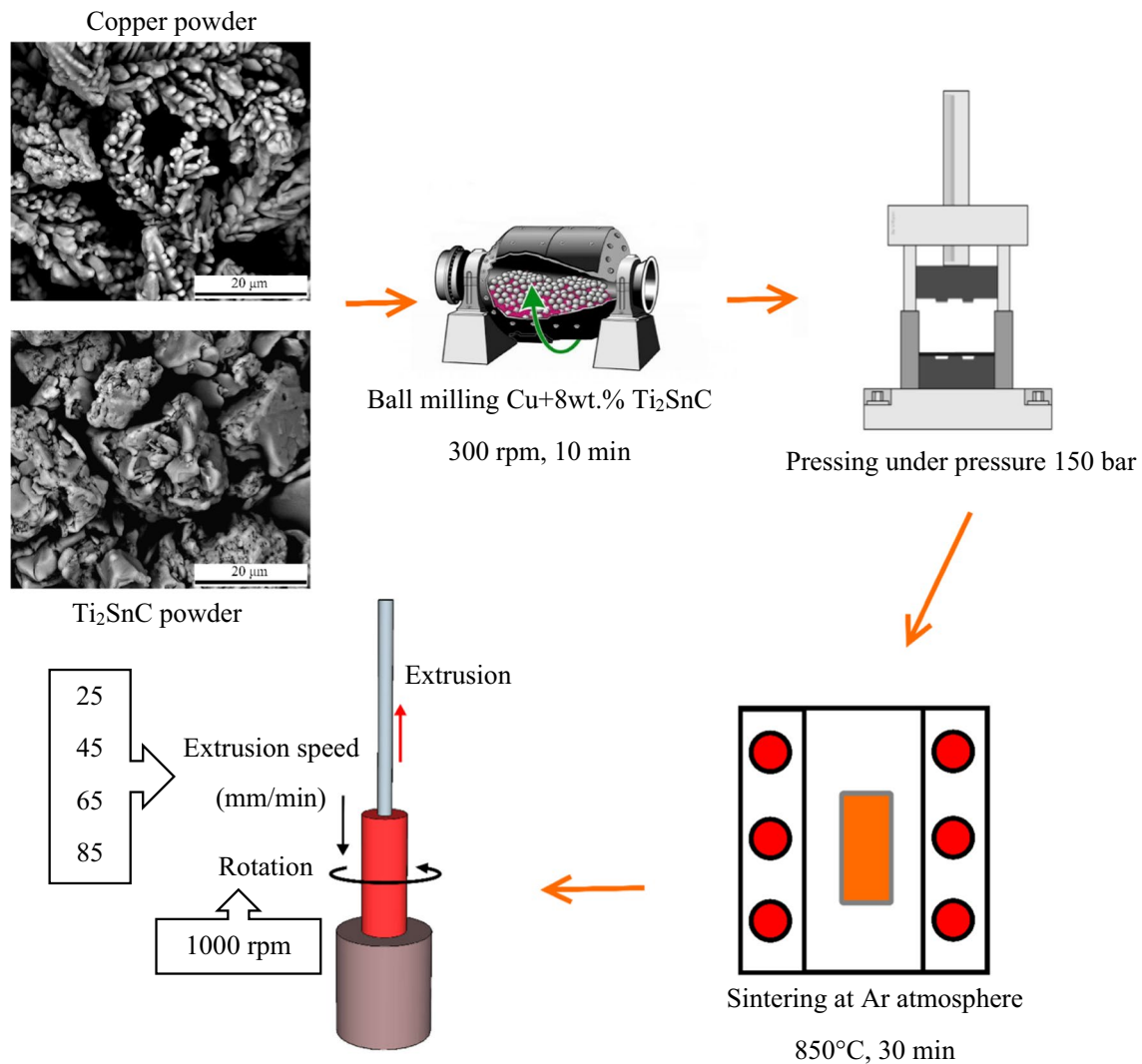


**Fig. 1** Schematic view of Cu–Ti<sub>2</sub>SnC composite wire fabrication by FSBE process

**Table 1** The FSBE processed sample labeling

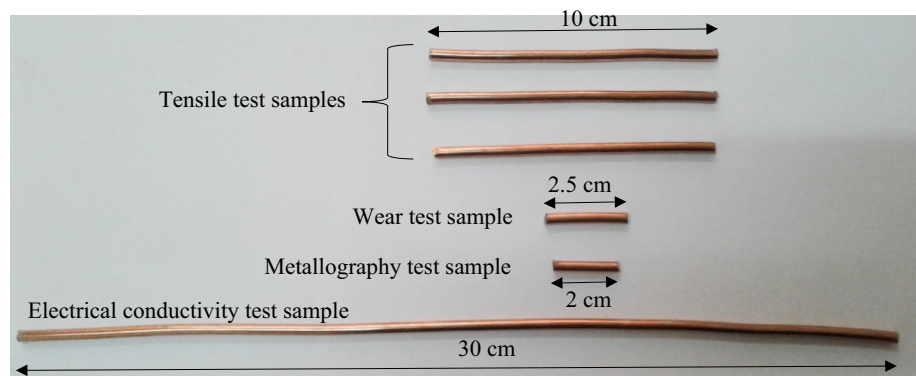
Sample label	Rotational speed (rpm)	Traverse speed (mm/min)	Reinforcement
Sample C-25	1000	25	Ti <sub>2</sub> SnC
Sample C-45	1000	45	Ti <sub>2</sub> SnC
Sample C-65	1000	65	Ti <sub>2</sub> SnC
Sample C-85	1000	85	Ti <sub>2</sub> SnC
Sample W-85	1000	85	–

### 3 Results and discussion

Figure 3 shows the optical microscopy microstructure of different samples. Figure 3a demonstrates the microstructure of the primary composite after sintering and before

the extrusion process. The microstructure contains a high percentage of porosity, which can be attributed to insufficient sintering time and temperature. Unfortunately, it is not possible to increase the time and temperature of the sintering process due to the possibility of the MAX phase decomposition [18]. Figure 3b–e depicts the microstructure of the composite after extrusion. The percentage of porosity decreases to a great extent. Importantly, by increasing the extrusion speed and applying more strain to the microstructure, the amount of agglomeration of the MAX phase decreased and the distribution of particles became more uniform. As shown, a layered structure was formed in the surface areas of the composite by reducing the extrusion speed. However, the grain size difference can be seen in the surface and central areas of the wire, in such a way that the grain size decreased by moving toward the surface areas of the wire. According to other studies [19–22], in the FSBE,

**Fig. 2** Dimension of different samples prepared to check the microstructure, mechanical properties, wear resistance, and electrical conductivity



the plastic strain and temperature are higher in the surface areas than in the central areas of the wire. Considering that the FSBE process has thermomechanical nature, recrystallized grains can be formed in the structure under the influence of heat and plastic deformation. The two factors of temperature and plastic strain are effective in the grain size of the recrystallized microstructure [23]. Here, it was observed that with increasing temperature and decreasing plastic strain, grain size increased. The reverse trend in the grain size was observed when the temperature decreased and the plastic strain increased. Since the grain size at the surface areas was smaller than the central areas of the wire, it can be said that the effect of plastic strain is effective in the formation of finer grains in the surface areas. This is while as shown in Fig. 4, the average grain size decreased with increasing extrusion speed. According to the experimental results of temperature measurement, the maximum temperature measured during the extrusion of the samples C-25, C-45, C-65, C-85, and W-85 is 861, 852, 824, 785, and 753 °C, respectively. The decrease in average grain size with decreasing temperature may be related to less opportunity for the growth of recrystallized grains as well as a more uniform distribution of reinforcing particles in the extruded wire that act as barriers to grain boundary movement.

The X-ray diffraction results of different samples are shown in Fig. 5. Except for the sample without reinforcement, copper peaks, MAX phase, and  $\text{Cu}_{81}\text{Sn}_{22}$  phase are observed in all composite samples. The peak  $\text{Cu}_{81}\text{Sn}_{22}$  phase in the unprocessed sample shows that due to the application of heat during the sintering process, part of the tin entered the copper matrix and formed the  $\text{Cu}_{81}\text{Sn}_{22}$  phase. Also, in the processed samples, it can be said that by applying heat and plastic deformation, tin can diffuse into copper, and as a result, this phase has been formed. Quantitative phase analysis taking into account the ratio of peak intensities shows that the value of this phase in the samples C-25, C-45, C-65, and C-85 is 1.0, 0.8, 0.7, and 0.5, respectively. It seems that by increasing the extrusion speed and decreasing the temperature during the FSBE process, the amount of  $\text{Cu}_{81}\text{Sn}_{22}$  phase decreased. This observation could be related to the

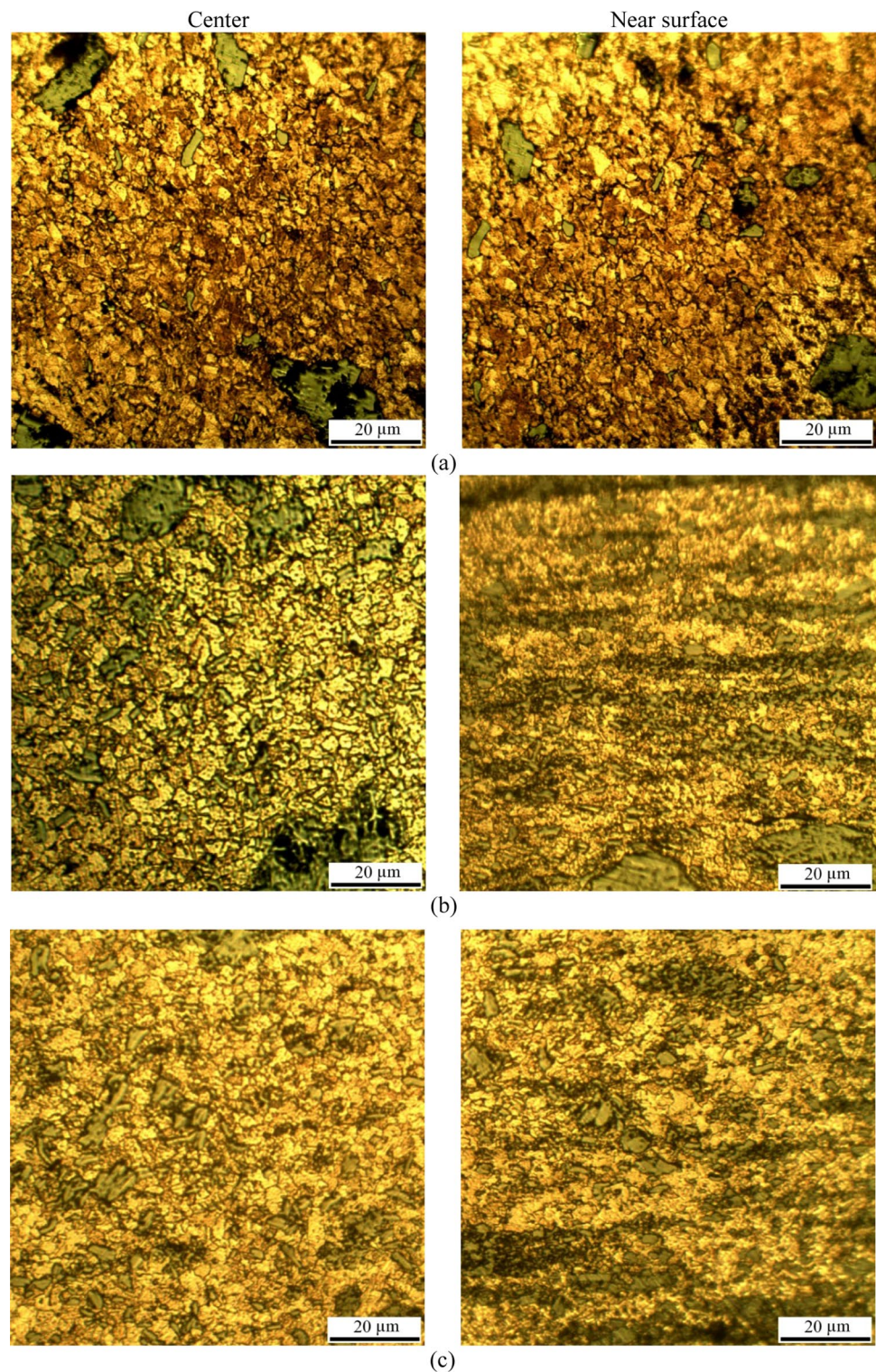
reduction of heat and plastic deformation during the FSBE process providing less diffusion opportunity for the formation of this phase. Figure 6 demonstrates the accumulated strain value of the extruded samples. In the extruded samples, as the extrusion speed increased from 25 to 85 mm/min, the accumulated strain decreased from 0.0093 to 0.0057 due to the application of less plastic strain. Therefore, the reduction of diffusion opportunity due to reduced plastic strain and temperature with increasing extrusion speed was not far from expected.

Figure 7 displays the SEM images of different samples. Also, Fig. 8 and Table 2 present the EDS analysis of different points. As shown, with the increase in extrusion speed, the distribution of reinforcing particles became more uniform and the un-bonded regions (as shown by yellow arrows) decreased. In addition, the distribution of the reactive layer became more uniform after the extrusion process. Figure 9 shows the distribution of elements around the MAX phase in samples C-25 and C-85. As shown, the distribution of tin occurred uniformly around the MAX phase. The analysis of the reactive layer shows a significant percentage of tin in this layer. According to other sources [18], this reactive layer is a solid solution of  $\text{Cu}(\text{Sn})$ , which is also reported in large quantities of tin the  $\text{Cu}_3\text{Sn}$  can form in the microstructure. According to the ratio of copper and tin in the reaction layer, this layer is probably the  $\text{Cu}_{81}\text{Sn}_{22}$  phase. However, with increasing rotation speed, the possibility of the formation of particles containing Ti and C increased. Other studies [18] introduced these particles as  $\text{TiC}_x$ , suggesting that the formation of these particles, although increases hardness, causes the electrical conductivity to decline.

Figure 10 shows the hardness profile as well as the average hardness of different samples. As shown, the hardness increased with the addition of the  $\text{Ti}_2\text{SnC}$  reinforcement. The average hardness of the composite wire compared to the wire without reinforcement increased by a minimum of 98%. It should be noted that with the increase in the extrusion speed, the average hardness increased and the hardness deviation decreased. The decrease in hardness deviation and the increase in average hardness are related to the more uniform



**Fig. 3** Optical microscopy image of microstructure of **a** Cu–Ti<sub>2</sub>SnC composite before FSBE, **b** sample C-25, **c** sample C-45, **d** sample C-65, **e** sample C-85, **f** sample W-85

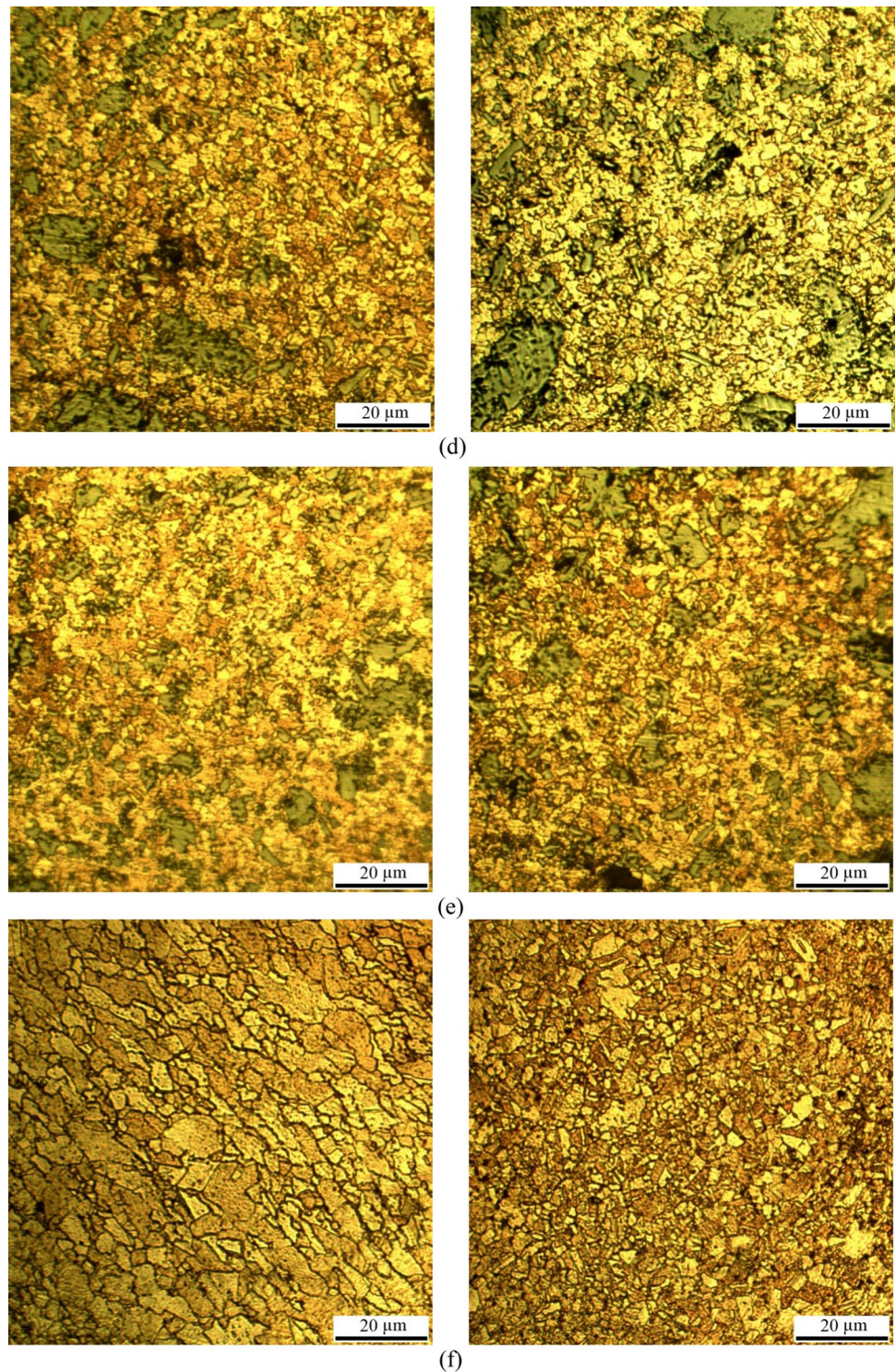


distribution of MAX reinforcement as well as the smaller grain size in the copper matrix, respectively. As shown, the hardness difference between the center and the surrounding of the wire decreased with the increase in the extrusion speed. The difference in hardness in the central areas and edges of the wire can be related to the changes in the grain

size of these two areas, the difference in the distribution of particles in the central areas and the edges of the wire, and more plastic strain in the surface areas of the wire. It should be noted that higher plastic strain values in the surface areas of the wire in the FSBE process have also been reported [4, 19–22]. More plastic strain in the edge of the wire during



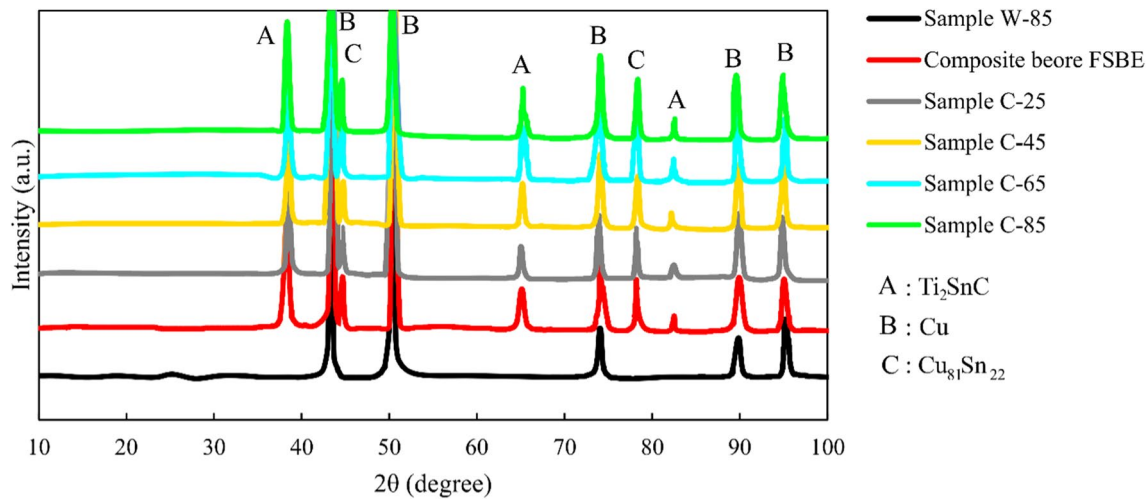
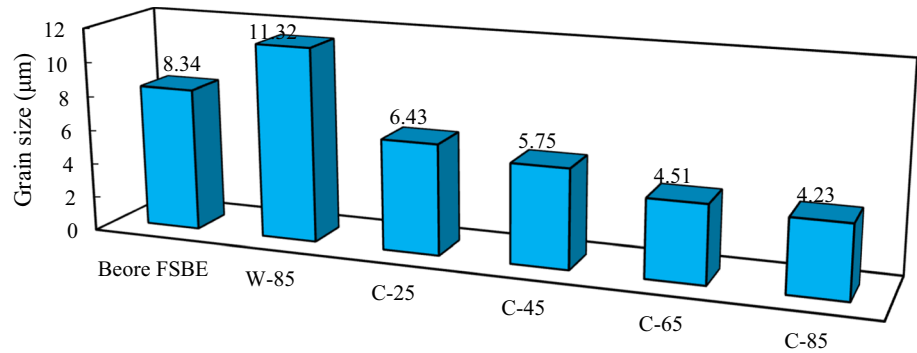
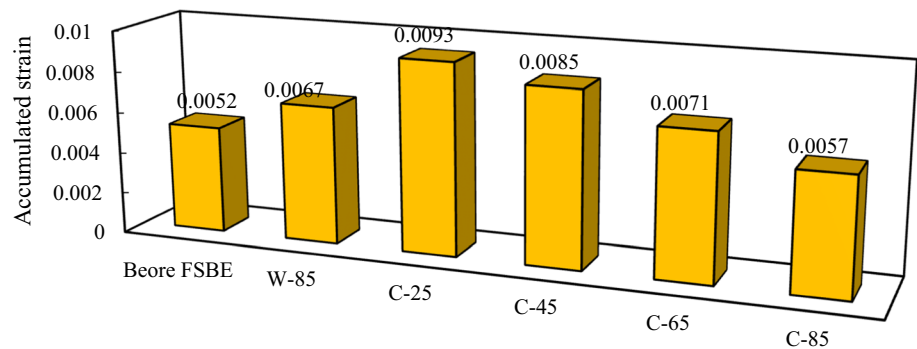
Fig. 3 (continued)



the extrusion process compared to the central areas causes an increase in the density of dislocations and residual stress in the edge areas, thus increasing the hardness in the edge areas of the wire compared to the central areas of the wire.

The stress–strain diagram of different samples along with changes in yield strength, ultimate tensile strength (UTS), and elongation of different samples are shown in Fig. 11.

With the addition of the MAX phase, the yield strength and UTS increased by at least 118 and 24%, respectively, but the elongation showed a minimum decrease of 46% compared to the wire without reinforcement. The increase in strength created in the composite wire is related to the activation of different strengthening mechanisms, which will be explained further. By increasing the extrusion speed, the maximum

**Fig. 4** The grain size distribution of different samples**Fig. 5** X-ray diffraction pattern of different samples**Fig. 6** The accumulated strain of different samples

strength and elongation increased. The increase in strength and elongation with the increase in extrusion speed is related to the improvement of the quality of the  $\text{Ti}_2\text{SnC}$ -Cu interface and the more uniform distribution of reinforcing particles in the copper matrix.

Given the reinforcement size used in this study, multiple strengthening mechanisms are effective in the strengthening of metal matrix composites: solid solution strengthening, load transfer [24], grain refinement [25], and thermal

mismatch [26, 27]. Although solid solution at the interface of Cu- $\text{Ti}_2\text{SnC}$  can affect the strength of the composites through the solid solution strengthening mechanism, it should be noted that most of the Sn in the copper matrix formed the  $\text{Cu}_{81}\text{Sn}_{22}$  phase. In this condition, the contribution of this mechanism in the strengthening of the composite can decline. The load transfer mechanism can be considered in the Cu- $\text{Ti}_2\text{SnC}$  composite in the condition that a relatively strong bond is formed between the matrix and the



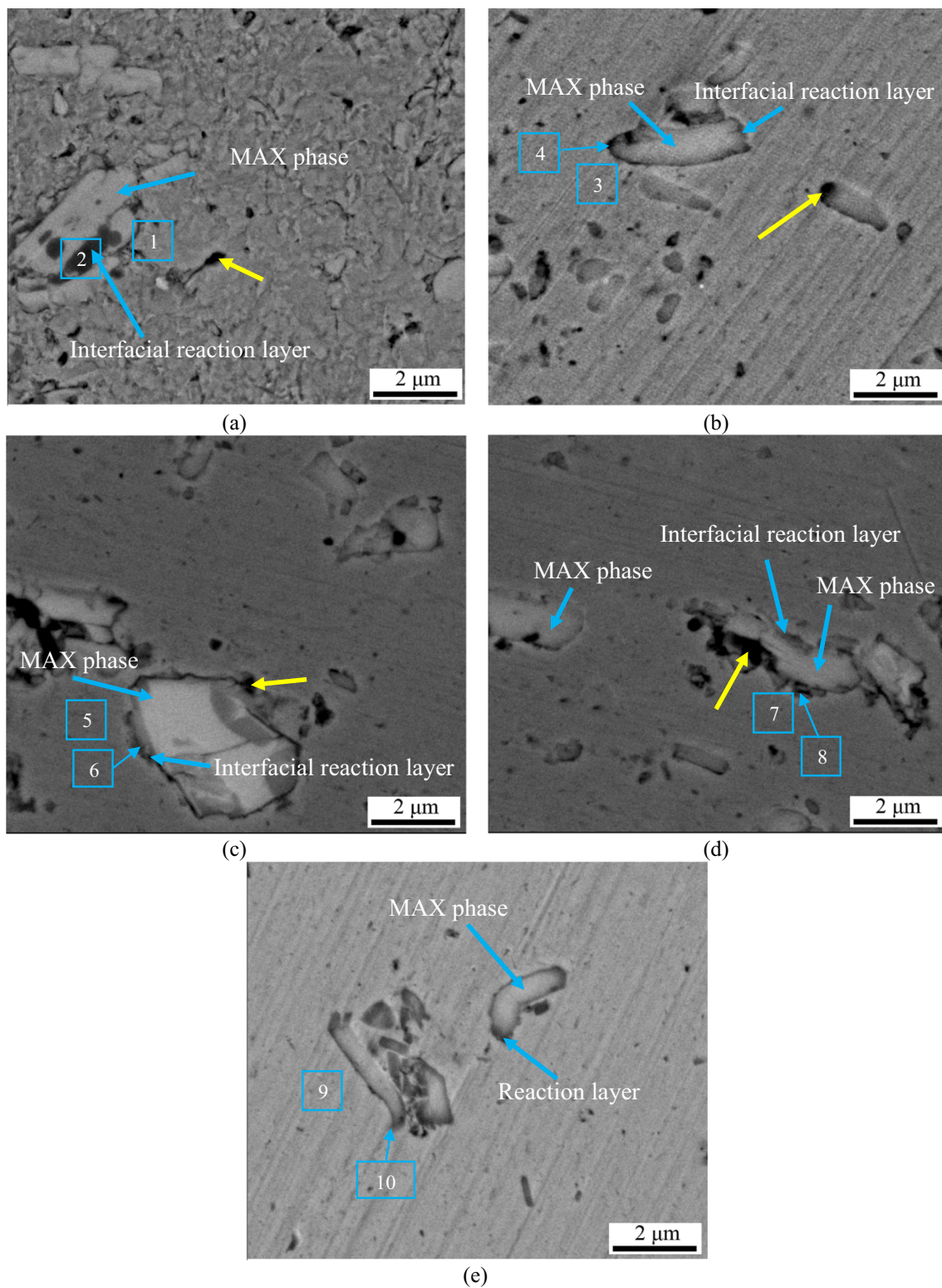


**Fig. 7** SEM micrograph of **a** Cu-Ti<sub>2</sub>SnC composite before FSBE, **b** sample C-25, **c** sample C-45, **d** sample C-65, **e** sample C-85

reinforcing particles. The microstructural analysis indicated that by increasing the extrusion speed up to 85 mm/min, the quality of the interface improved. Therefore, it can be

expected that the contribution of the load transfer strengthening mechanism will be enhanced by increasing extrusion speed. The more uniform distribution of Ti<sub>2</sub>SnC particles in



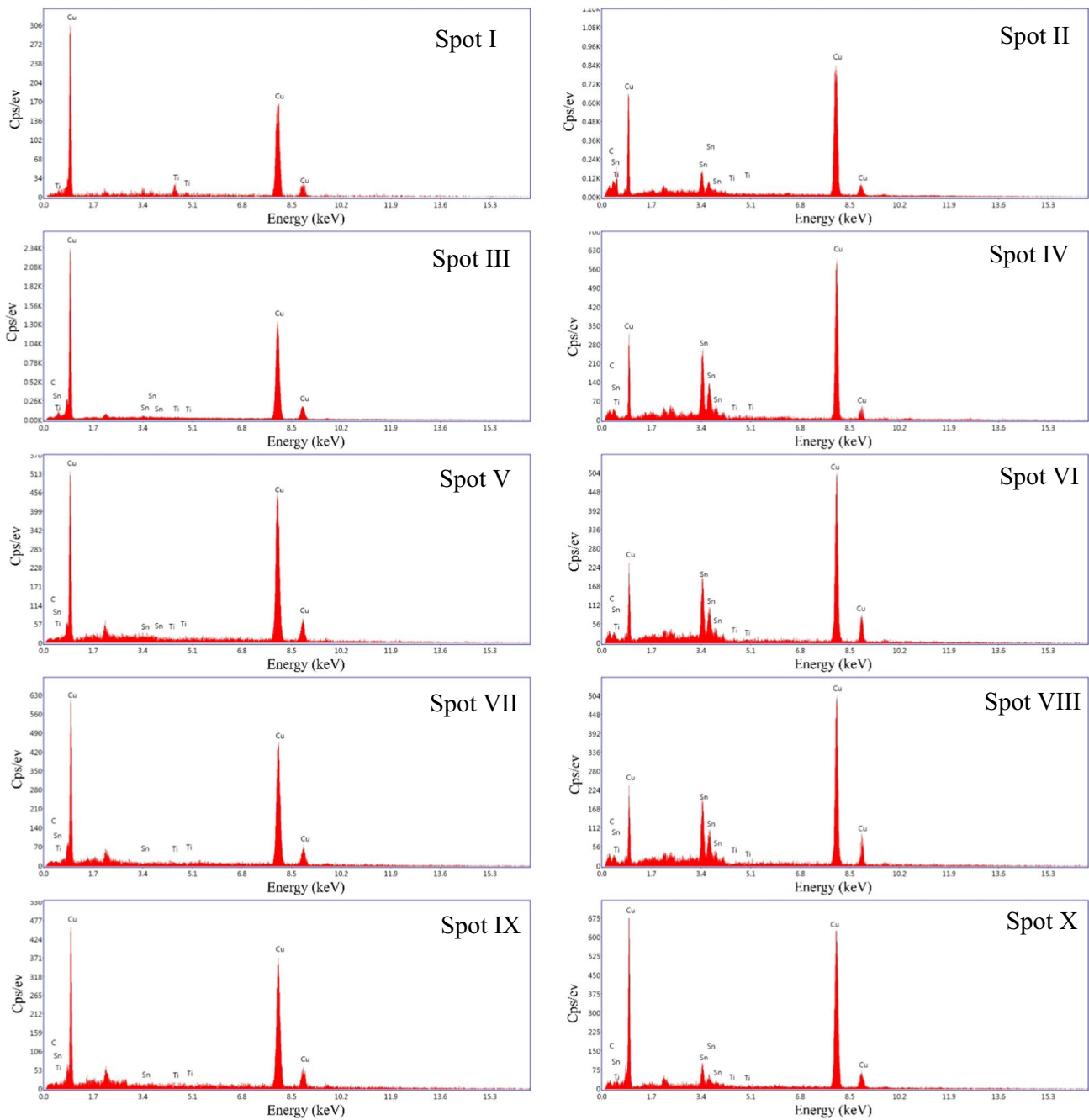
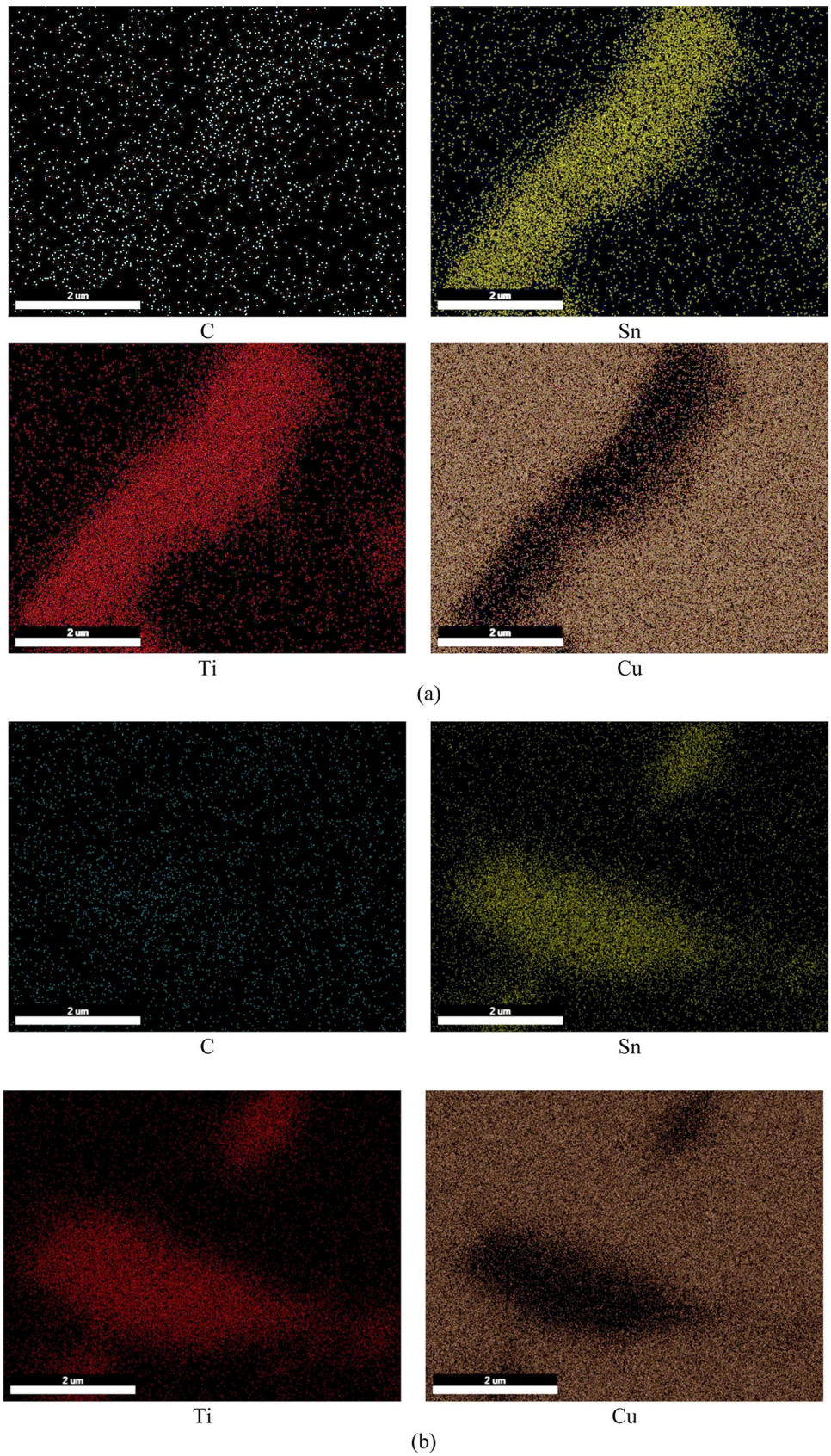


Fig. 8 EDS analysis of different points marked in Fig. 7

Table 2 Chemical composition of different points marked in Fig. 7

Element	Position									
	1	2	3	4	5	6	7	8	9	10
Ti (at. %)	0.1	5.4	0.12	4.96	0.15	5.32	0.87	6.32	0.32	2.05
Sn (at. %)	0.09	21.32	0.09	21.09	0.98	19.23	0.09	24.12	0.18	23.12
C (at. %)	0.05	1.12	0.1	1.09	0.09	1.18	0.11	0.92	0.07	0.69
Cu (at. %)	99.76	72.16	99.69	72.86	98.78	74.27	98.93	68.64	99.43	74.14

**Fig. 9** The distribution of elements around the MAX phase in the samples: **a** C-25, and **b** C-85



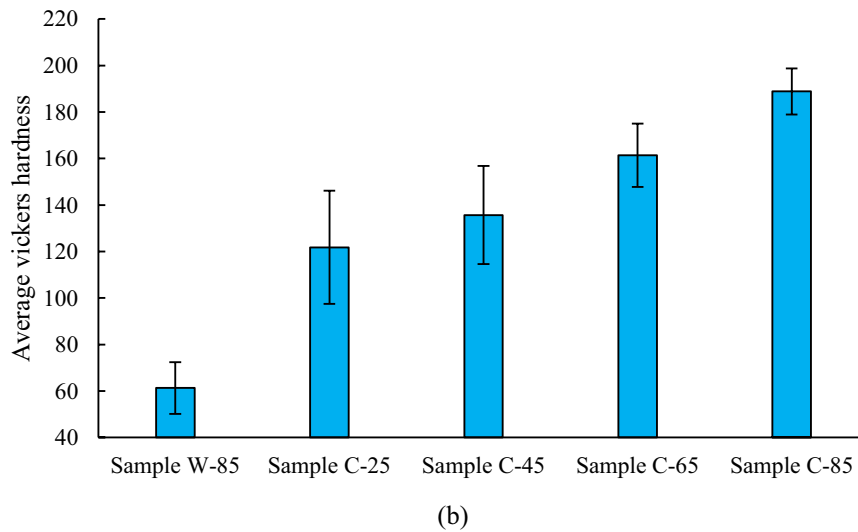
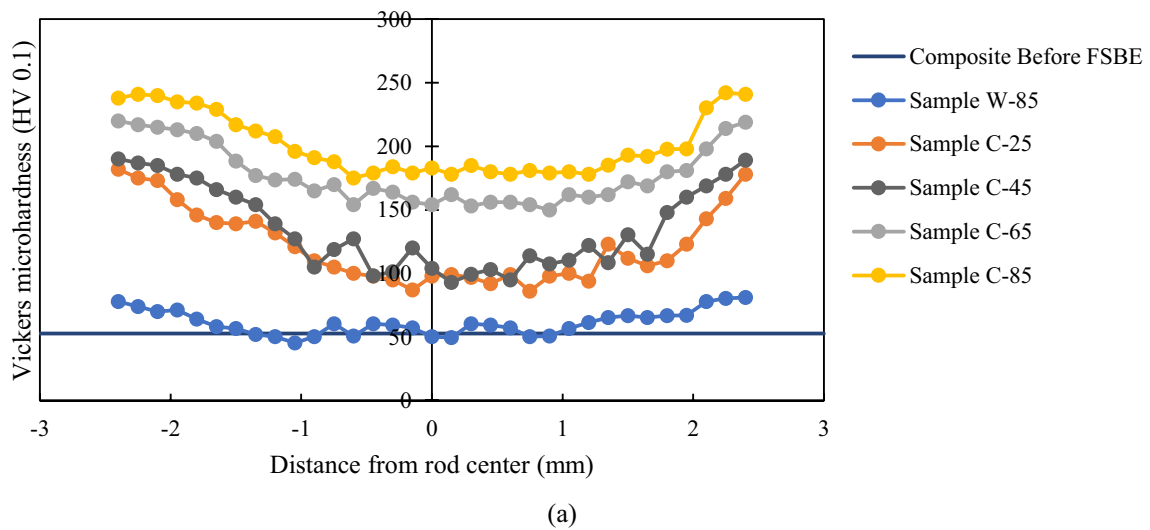
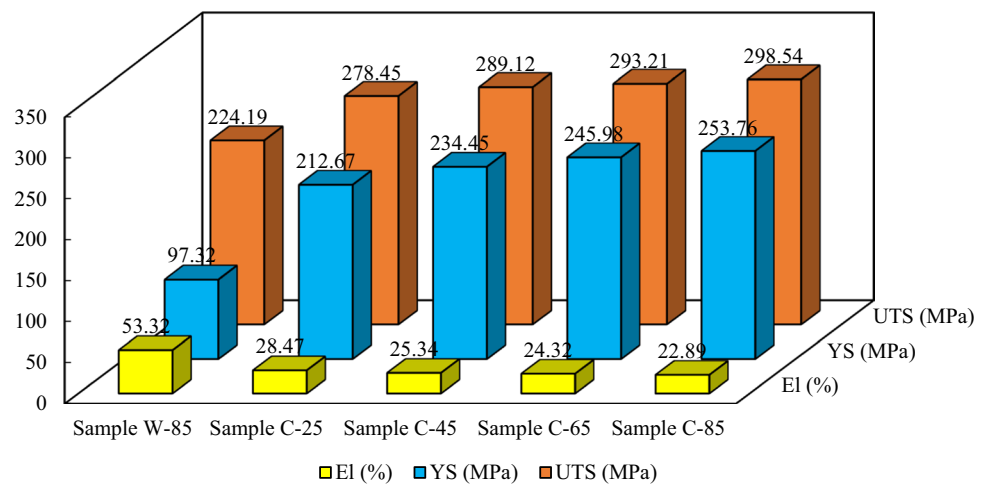


Fig. 10 a Vickers microhardness profile and b average hardness of different samples

Fig. 11 The tensile test property of different samples





the copper matrix results in grain refinement during dynamic recrystallization and can prevent the growth of recrystallized grains by the Zener pinning effect [28]. By decreasing the grain size with increasing extrusion speed, the strength of the composite can increase according to the Hall–Patch relationship [29].

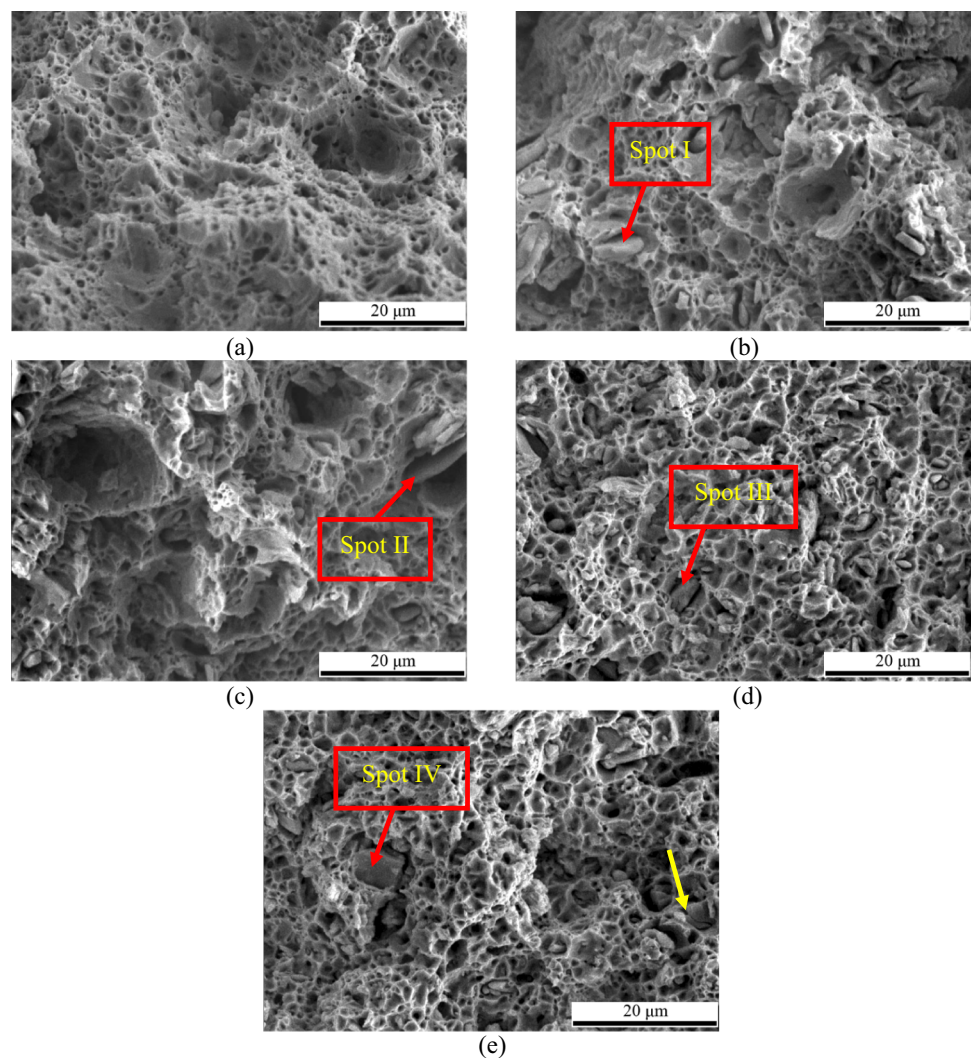
Also, the mismatch of the thermal expansion and modulus of elasticity coefficients between the copper matrix and  $Ti_2SnC$  particles can act as a strengthening mechanism by the formation of geometrically necessary dislocations (GNDs) [11, 25, 30]. Increasing the extrusion speed increases the cooling rate of the composite wire during FSBE. In this condition, the higher the formation of GND in the copper matrix [31], the higher the strength of the composite.

Figure 12 shows the SEM images of the fracture surfaces of different samples. Also, the EDS analysis of particles in the fracture surface is reported in Fig. 13. The presence of dimples and micro voids in the fracture surface of the

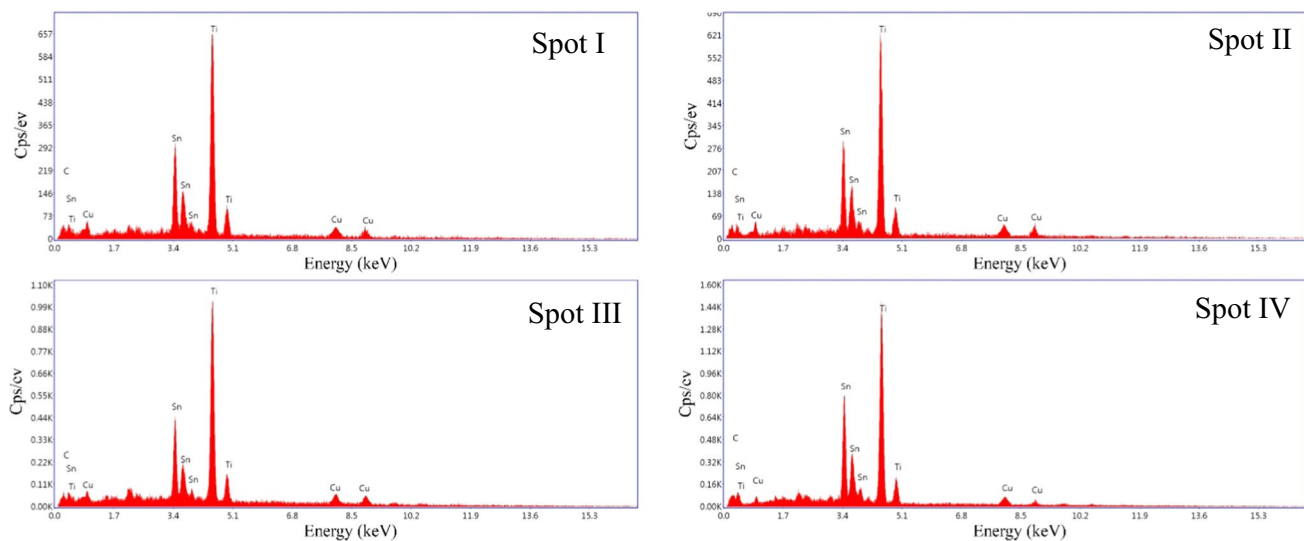
extruded wires shows ductile fracture nature [32]. The presence of the dimples indicates that the matrix underwent significant plastic deformation before the fracture. Figures 12a–d relates to the composite wires, and Fig. 12e shows the pure copper wire. The reinforcement particle shown by the red arrows is entrapped in the hole of the matrix. These particles have a crucial role in inhibiting of propagation of cracks so that higher tensile strength is obtained [33]. Also, broken  $Ti_2SnC$  in the fracture surface of sample C-85, which is shown by the yellow arrows, indicates the proper load transfer role during the tensile test.

Figure 14 shows the electrical conductivity of the extruded wires. Electrical conductivity of metals induced by the motion of free electrons. The factors affecting the movement of electrons are obstacles such as grain boundaries, dislocations, and secondary phase particles. Another important factor that affects the mobility of electrons is the presence of the porosities at the interface of the matrix and reinforcement, causing the electrons to be scattered in these

**Fig. 12** SEM image of fracture surface of **a** sample W-85, **b** sample C-25, **c** sample C-45, **d** sample C-65, **e** sample C-85

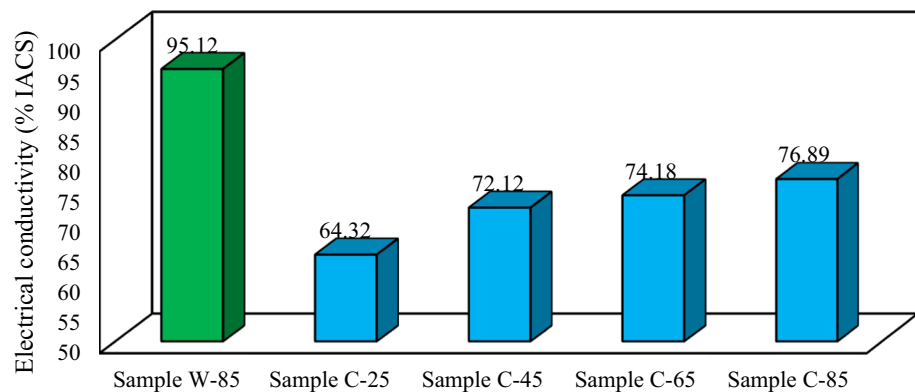






**Fig. 13** EDS analysis of different points marked in Fig. 12

**Fig. 14** The electrical conductivity of different samples



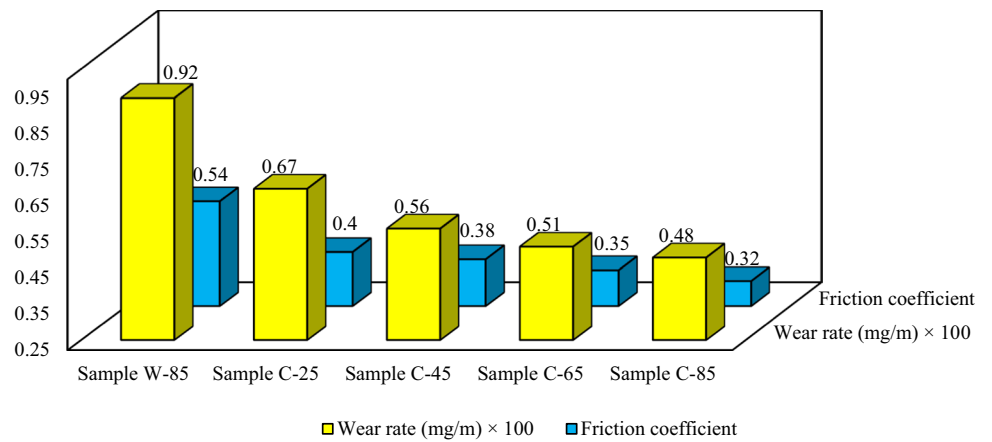
zones [34]. By applying the FSBE process, the dislocation density increases and the presence of the reinforcement create interfaces at the copper matrix. These factors promote electron scattering. The electrical conductivity of the composite wires is 64.32, 72.12, 74.18, and 76.89% IACS for the samples C-25, C-45, C-65, and C-85, respectively. The electrical conductivity of W-85 (the reinforcement-free sample) is 95.12% IASC.

To predict the electrical conductivity of Cu–8 wt%  $\text{Ti}_2\text{SnC}$  composite, the rule of mixtures is assumed. Electrical conductivity values of pure copper and  $\text{Ti}_2\text{SnC}$  are considered as 97.12 and 58.00% IASC, respectively. Since all composite wires have the same volume percent, the predicted electrical conductivity is 93.21% IASC. The difference in the electrical conductivity values between the composite wires is insignificant. The formation porosity around the reinforcement, formation reaction phase, and grain boundaries can cause the electrical conductivity of composite wires to be less than predicted. By increasing the extrusion speed to

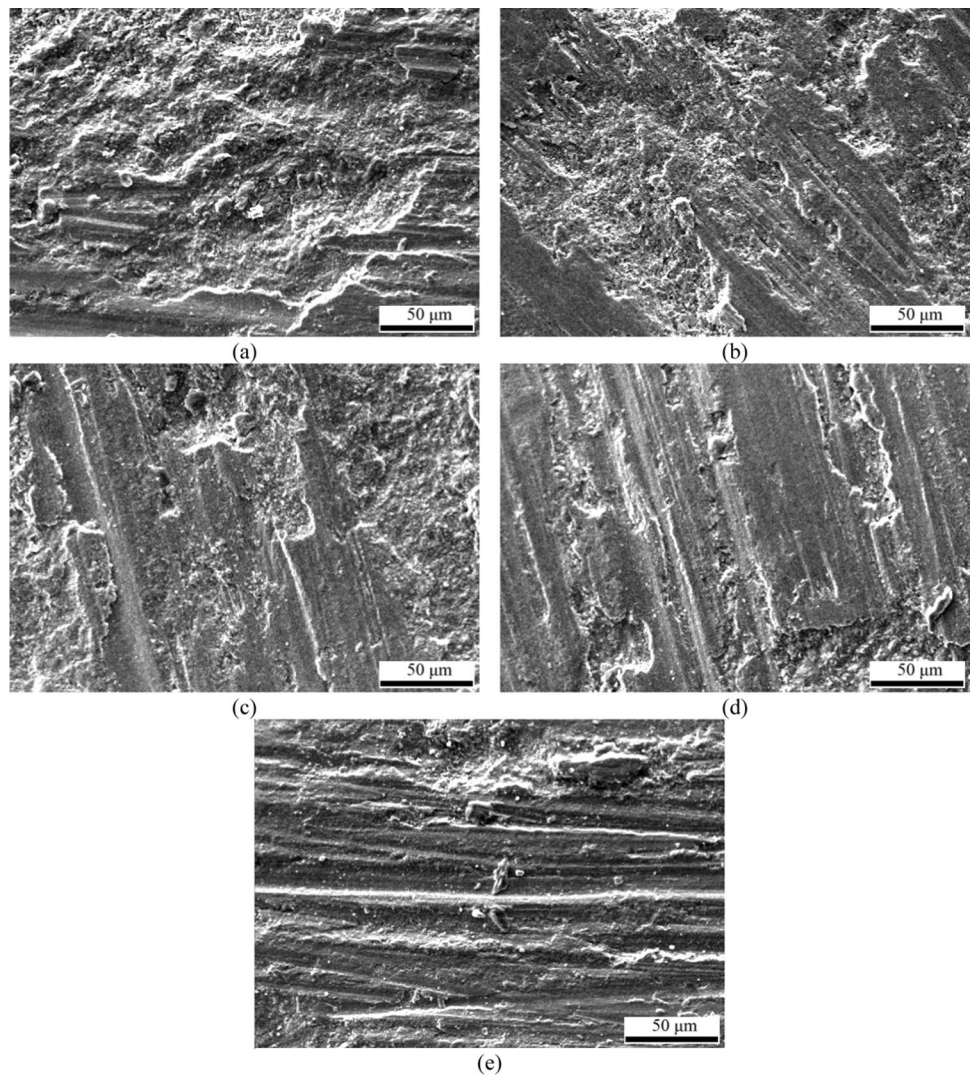
85 mm/min, less porosity and less reaction phase can cause an increment in the amount of electrical conductivity. Furthermore, as said in the microstructure section the formation of  $\text{TiC}_x$  can reduce the electrical conductivity. It should be considered that although sample C-85 has a smaller grain size than others, the effect of porosities, reaction phase, and interface quality of MAX phase and matrix have a dominant effect on electrical conductivity.

Figure 15 shows the wear rate and friction coefficient of the extruded wires. The wear rate and friction coefficient of the sample C-85 reinforcement free are 0.0092 mg/m and 0.54, respectively. Figure 16 shows the SEM images of the wear surface of the extruded samples. The severe plastic deformation and severe material removal of the pure copper on the wear surface, according to Fig. 16a, is because of the low hardness. Also, Fig. 17 indicates the copper stuck on the surface of the wear disk that confirms the adhesive wear mechanism in the pure copper wire. Improvement in the hardness of the composite wires, as a dominative role,

**Fig. 15** The wear rate and friction coefficient of different samples



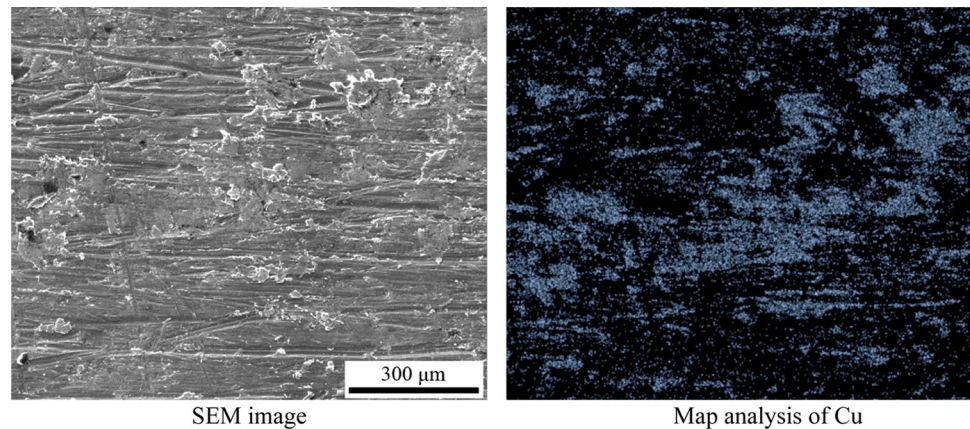
**Fig. 16** SEM image of wear surface of **a** sample W-85, **b** sample C-25, **c** sample C-45, **d** sample C-65, **e** sample C-85



causes the friction coefficient to decrease and the friction coefficient from 0.54 for the pure copper reaches 0.40, 0.38, 0.35, and 0.32 for the samples C-25, C-45, C-65, and C-85, respectively. The wear resistance of the composite wires

improved due to the increment of the hardness that impedes the plastic deformation of the copper matrix. Also, improved wear resistance by increasing hardness was reported by other studies [1, 35]. The maximum wear rate between composite

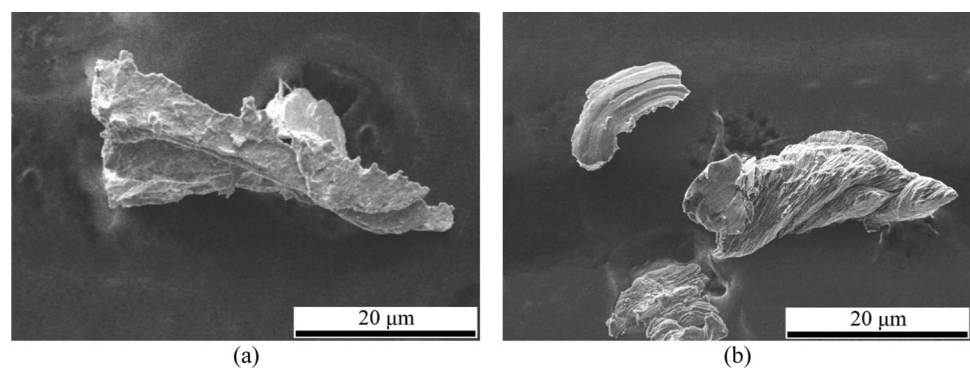
**Fig. 17** The EDS map analysis of the wear test disk for pure Cu wire



wires was related to C-25 with a value of 0.0067 mg/m, and the minimum wear rate was related to C-85 with a value of 0.0048 mg/m. Among the composite wires, sample C-25 had the highest depth of wear scar due to the highest amount of porosities and thus the worst interfacial bonding. By increasing the extrusion speed from 25 to 85 mm/min, the wear scar depth decreased, and abrasive wear mechanism contribution increased due to the improvement of the MAX phase/Cu matrix interface quality and distribution of MAX phases. As shown, in the wear surface of different samples with a decrease in the hardness of the coating, deeper grooves have been created compared to the samples with higher hardness. These cases, along with the presence of plastic deformation on the surface of the sample, indicate wear with an adhesive mechanism [36, 37]. The similar results achieved in lower amount of  $Ti_2SnC$  reinforcement [38]. The grooves created on the surface indicate the abrasive wear mechanism. This mechanism is applied in different ways at different times of the test. Thus, in the beginning, there was two-body abrasive wear, but with the increasing wear time and the particles separating from the wear surface and their oxidation over time, these particles become hard during wear, and these hard particles can cause the three-body abrasive wear mechanism.

Figure 18 shows the debris of samples W-85 and C-85. Material removal occurs due to delamination causing the formation of a microcrack. Debonding of reinforced particles results in a high wear rate of material as softer matrix comes in direct contact and also debonded particles are trapped during sliding which causes abrasive wear through the three-body wear mechanism. The formation of wear debris results in third-body abrasion and great plastic deformation under severe conditions [39]. Microcracks on the surface of debris indicate the resistance offered by the embedded particles once detached leaves crack in the surface. A change in the size and morphology of the wear debris with increasing reinforcement is clearly visible. The size of flakes increases more substantially, which indicates that the matrix is softer in the absence of reinforcement and causes the transition from mild to severe wear. These wear debris indicate that the adhesive wear dominates in the sliding direction during wear. Given the adhesive nature of wire without reinforcement, metal is chipped out in the form of flakes as debris. Large-size debris in samples without reinforcement suggests that the material was removed at a higher rate, which reduced wear resistance.

**Fig. 18** The wear debris of **a** sample W-85 and **b** sample C-85



## 4 Conclusion

Here, the effects of extrusion speed in the friction stir back extrusion on microstructure, mechanical, electrical, and wear properties of Cu–Ti<sub>2</sub>SnC composite were investigated. The most significant results were:

- By increasing the extrusion speed and applying more strain to the microstructure, the amount of agglomeration of the Ti<sub>2</sub>SnC MAX phase decreases and the distribution of particles becomes more uniform.
- The grain size difference can be seen in the surface and central areas of the wire, in such a way that the grain size decreases by moving toward the surface areas of the wire. Also, the average grain size decreases from  $6.43 \pm 1.02$  to  $4.23 \pm 0.95$   $\mu\text{m}$  with increasing extrusion speed from 25 to 85 mm/min.
- The average hardness of the composite wire compared to the wire without reinforcement has a minimum 98% increase. With the increase of the extrusion speed from 25 to 85 mm/min, the average hardness increases from 121.78 to 188.84 HV0.1.
- With the addition of the Ti<sub>2</sub>SnC MAX phase, the yield strength and UTS have increased by at least 118 and 24%, respectively, but the elongation shows a decrease of at least 46% compared to the wire without reinforcement.
- By the addition of 8 wt% Ti<sub>2</sub>SnC reinforcement and performing FSBE with a rotational speed of 1000 rpm and a traverse speed of 85 mm/min, the yield strength, UTS, and wear resistance increased by 160, 33, and 47%, respectively, compared to the un-reinforced copper matrix.
- Reducing the extrusion traverse speed from 85 to 25 mm/min decreased the friction coefficient and wear rate by 28% and 20%, respectively.

## References

1. Moharami A (2020) Improving the dry sliding-wear resistance of as-cast Cu-10Sn-1P alloy through accumulative back extrusion (ABE) process. *J Market Res* 9:10091–10096
2. Akbarpour M, Salahi E, Hesari FA, Yoon E, Kim H, Simchi A (2013) Microstructural development and mechanical properties of nanostructured copper reinforced with SiC nanoparticles. *Mater Sci Eng A* 568:33–39
3. Akhtar F, Askari SJ, Shah KA, Du X, Guo S (2009) Microstructure, mechanical properties, electrical conductivity and wear behavior of high volume TiC reinforced Cu-matrix composites. *Mater Charact* 60:327–336
4. Akbari M, Asadi P (2021) Simulation and experimental investigation of multi-walled carbon nanotubes/aluminum composite fabrication using friction stir processing. *Proc Inst Mech Eng Part E J Process Mech Eng* 235:2165–2179
5. Akbari M, Asadi P, Asiabarak HR (2022) Investigation of wear and microstructural properties of A356/TiC composites fabricated by FSP. *Surf Rev Lett (SRL)* 29:1–10
6. Ritasalo R, Liua X, Söderberg O, Keski-Honkola A, Pitkänen V, Hannula S (2011) The microstructural effects on the mechanical and thermal properties of pulsed electric current sintered Cu–Al<sub>2</sub>O<sub>3</sub> composites. *Procedia Eng* 10:124–129
7. James J, Annamalai AR, Muthuchamy A, Jen C-P (2021) Effect of wettability and uniform distribution of reinforcement particle on mechanical property (Tensile) in aluminum metal matrix composite—a review. *Nanomaterials* 11:2230
8. Chen J, Niu P, Wei T, Hao L, Liu Y, Wang X, Peng Y (2015) Fabrication and mechanical properties of AlCoNiCrFe high-entropy alloy particle reinforced Cu matrix composites. *J Alloy Compd* 649:630–634
9. Low I-M (2013) MAX phases and ultra-high temperature ceramics for extreme environments. IGI Global, New York
10. Wu J, Zhou Y, Yan C (2005) Mechanical and electrical properties of Ti<sub>2</sub>SnC dispersion-strengthened copper. *MEKU* 96:847–852
11. Sun Z (2011) Progress in research and development on MAX phases: a family of layered ternary compounds. *Int Mater Rev* 56:143–166
12. Wu JY, Chai K (2007) Strengthening of Cu–Ti<sub>2</sub>SnC composites due to microstructural changes in the material. In: *Key engineering materials*, Trans Tech Publ, pp 429–432
13. Wu J, Zhou Y, Wang J (2006) Tribological behavior of Ti<sub>2</sub>SnC particulate reinforced copper matrix composites. *Mater Sci Eng A* 422:266–271
14. Wu J, Zhou Y, Wang J, Wang W, Yan C (2022) Interfacial reaction between Cu and Ti<sub>2</sub>SnC during processing of Cu–Ti<sub>2</sub>SnC composite. *Int J Mater Res* 96:1314–1320
15. Zhang F, Yan F, Chen T, Li X, Wang Z (2021) Investigating the effect of load on tribological behaviour of Cu composite reinforced with Ti<sub>2</sub>SnC particles. *Ind Lubric Tribol* 73:207–214
16. Asadi P, Akbari M, Kohantorabi O, Peyghami M, Aliha MRM, Salehi SM, Asiabarak HR, Berto F (2022) Characterization of the influence of rotational and traverse speeds on the mechanical and microstructural properties of wires produced by the FSBE method. *Strength Mater* 54:318–330
17. Li X, Zhou C, Overman N, Ma X, Canfield N, Kappagantula K, Schroth J, Grant G (2021) Copper carbon composite wire with a uniform carbon dispersion made by friction extrusion. *J Manuf Process* 65:397–406
18. Wu J, Zhou Y, Wang J, Wang W, Yan C (2005) Interfacial reaction between Cu and Ti<sub>2</sub>SnC during processing of Cu–Ti<sub>2</sub>SnC composite. *MEKU* 96:1314–1320
19. Asadi P, Akbari M (2021) Numerical modeling and experimental investigation of brass wire forming by friction stir back extrusion. *Int J Adv Manuf Technol* 116:3231–3245
20. Baffari D, Buffa G, Campanella D, Fratini L, Reynolds AP (2017) Process mechanics in friction stir extrusion of magnesium alloys chips through experiments and numerical simulation. *J Manuf Process* 29:41–49
21. Abdi Behnagh R, Samanta A, Agha Mohammad Pour M, Esmailzadeh P, Ding H (2019) Predicting microstructure evolution for friction stir extrusion using a cellular automaton method. *Model Simul Mater Sci Eng* 27:035006
22. Mehtedi ME, Forcellese A, Mancia T, Simoncini M, Spigarelli S (2019) A new sustainable direct solid state recycling of AA1090 aluminum alloy chips by means of friction stir back extrusion process. *Procedia CIRP* 79:638–643
23. Sadoun AM, Wagih A, Fathy A, Essa ARS (2019) Effect of tool pin side area ratio on temperature distribution in friction stir welding. *Results Phys* 15:102814



24. Tong W, Fang D, Bao C, Tan S, Liu Y, Li F, You X, Tao J, Bao R, Li C (2022) Enhancing mechanical properties of copper matrix composite by adding SiO<sub>2</sub> quantum dots reinforcement. *Vacuum* 195:110682
25. Cheng C, Song K, Mi X, Wu B, Xiao Z, Xie H, Zhou Y, Guo X, Liu H, Chen D (2020) Microstructural evolution and properties of Cu–20 wt% Ag alloy wire by multi-pass continuous drawing. *Nanotechnol Rev* 9:1359–1367
26. Wu Q, Miao W-S, Zhang Y-D, Gao H-J, Hui D (2020) Mechanical properties of nanomaterials: a review. *Nanotechnol Rev* 9:259–273
27. Lin H, Guo X, Song K, Feng J, Li S, Zhang X (2021) Synergistic strengthening mechanism of copper matrix composite reinforced with nano-Al<sub>2</sub>O<sub>3</sub> particles and micro-SiC whiskers. *Nanotechnol Rev* 10:62–72
28. Badran A, Alamro T, Bazuhair RW, El-Mawla AAG, El-Adben S, Fouly A (2022) Investigation of the mechanical behavior of synthesized Al6061/TiO<sub>2</sub> microcomposites using an innovative stir casting method. *Nanomaterials* 12:1646
29. Akbarpour MR, Salahi E, Alikhani Hesari F, Kim HS, Simchi A (2013) Effect of nanoparticle content on the microstructural and mechanical properties of nano-SiC dispersed bulk ultrafine-grained Cu matrix composites. *Mater Des* (1980–2015) 52:881–887
30. Bahador A, Umeda J, Hamzah E, Yusof F, Li X, Kondoh K (2020) Synergistic strengthening mechanisms of copper matrix composites with TiO<sub>2</sub> nanoparticles. *Mater Sci Eng A* 772:138797
31. Dai LH, Ling Z, Bai YL (2001) Size-dependent inelastic behavior of particle-reinforced metal–matrix composites. *Compos Sci Technol* 61:1057–1063
32. Nosewicz S, Bazarnik P, Clozel M, Kurpaska Ł, Jenczyk P, Jarząbek D, Chmielewski M, Romelczyk-Baishya B, Lewandowska M, Pakieła Z (2021) A multiscale experimental analysis of mechanical properties and deformation behavior of sintered copper–silicon carbide composites enhanced by high-pressure torsion. *Arch Civ Mech Eng* 21:131
33. Singh MK, Gautam RK (2017) Synthesis of copper metal matrix hybrid composites using stir casting technique and its mechanical, optical and electrical behaviours. *Trans Indian Inst Met* 70:2415–2428
34. Hidalgo-Manrique P, Lei X, Xu R, Zhou M, Kinloch IA, Young RJ (2019) Copper/graphene composites: a review. *J Mater Sci* 54:12236–12289
35. Moharrami A, Razaghian A, Paidar M, Šlapáková M, Ojo OO, Taghiabadi R (2020) Enhancing the mechanical and tribological properties of Mg<sub>2</sub>Si-rich aluminum alloys by multi-pass friction stir processing. *Mater Chem Phys* 250:123066
36. Markov D, Kelly D (2000) Mechanisms of adhesion-initiated catastrophic wear: pure sliding. *Wear* 239:189–210
37. Zhan Y, Zhang G (2006) The role of graphite particles in the high-temperature wear of copper hybrid composites against steel. *Mater Des* 27:79–84
38. Jahani A, Jamshidi Aval H, Rajabi M, Jamaati R (2023) Effects of Ti<sub>2</sub>SnC MAX phase on microstructure, mechanical, electrical, and wear properties of stir-extruded copper matrix composite. *Adv Eng Mater* 2201463
39. Savaşkan T, Bican O (2010) Dry sliding friction and wear properties of Al–25Zn–3Cu–(0–5) Si alloys in the as-cast and heat-treated conditions. *Tribol Lett* 40:327–336

**Publisher's Note** Springer Nature remains neutral with regard to jurisdictional claims in published maps and institutional affiliations.

Springer Nature or its licensor (e.g. a society or other partner) holds exclusive rights to this article under a publishing agreement with the author(s) or other rightsholder(s); author self-archiving of the accepted manuscript version of this article is solely governed by the terms of such publishing agreement and applicable law.